NACA RM E56B29

RESEARCH MEMORANDUM

USE OF EFFECTIVE MOMENTUM THICKNESS IN DESCRIBING TURBINE ROTOR-BLADE LOSSES

By Warner L. Stewart, Warren J. Whitney, and James W. Miser

Lewis Flight Propulsion Laboratory
Cleveland, Ohio

NATIONAL ADVISORY COMMITTEE
FOR AERONAUTICS

WASHINGTON

May 14, 1956

NACA RM E56B29

NATIONAL ADVISORY COMMITTEE FOR AERONAUTICS

RESEARCH MEMORANDUM

USE OF EFFECTIVE MOMENTUM THICKNESS IN DESCRIBING TURBINE ROTOR-BLADE LOSSES

By Warner L. Stewart, Warren J. Whitney, and James W. Miser

SUMMARY

The use of an effective rotor-blade momentum thickness in describing rotor-blade loss characteristics is discussed herein. A derivation of the necessary equations is presented for obtaining this momentum thickness for given over-all turbine performance, stator performance, and rotor geometric quantities.

The effective rotor-blade momentum thickness was calculated for a series of transonic rotors previously investigated. The ratio of this thickness to the blade mean camber length is correlated with the sum of the design rotor-blade suction- and pressure-surface diffusion parameters. Comparison of this correlation with that obtained from low-speed two-dimensional cascade results showed similar slopes but higher values of momentum thickness for the rotors. Some of the possible reasons for this difference are the inability to measure rotor surface diffusions and the effects of velocity level, turbulence, and three-dimensional secondary flows.

INTRODUCTION

A study of the sources and significance of the various losses occurring within turbine blade rows is in progress at the NACA Lewis laboratory. Such information is necessary not only to aid in the design of efficient turbines, but also to indicate the direction of future research. The blade-row losses are described in reference 1 in terms of basic boundary-layer parameters. Because the blade exit momentum thickness is the most significant parameter in the determination of the blade loss (ref. 1), an estimation of the blade loss based on boundary-layer parameters depends on an accurate evaluation of the momentum-thickness parameter.

Application of boundary-layer parameters has been made in studying the loss characteristics of typical single-stage turbine stators (refs. 2 to 4, e.g.). Obtaining the necessary data was somewhat simplified in

that the wake surveys could easily be taken downstream of the blade row. Analysis of the results was also straightforward in that inlet conditions were uniform and known, and the stators operated with a large static-pressure drop so that there was very little, if any, diffusion on the blade surfaces. Thus surface diffusion was not considered to have any appreciable effect on the stator-blade loss.

The analysis of rotor loss characteristics is considerably more difficult in that rotors generally operate with considerably lower reaction resulting in higher blade surface diffusion as compared with that of stators. Thus, blade surface diffusion becomes a most important parameter in describing rotor losses. The study of rotor loss characteristics is then hampered by the difficulty in experimentally determining the blade diffusions. Further, effects of variations in rotor-inlet conditions due to stator wakes and secondary-flow cores, as well as secondary flows within the rotors themselves, make the analysis of rotor loss characteristics even more difficult. Finally, the inability to obtain accurate wake measurements behind rotors makes the determination of rotor loss characteristics very difficult.

In spite of these difficulties some attempts have been made to study the sources and significance of the losses occurring within rotors. In references 5 to 9 a series of transonic turbine rotors are investigated. These rotors were all designed for approximately the same speed, weight flow, and work output. A considerable variation in rotor solidity was covered resulting in a wide range of design suction- and pressure-surface diffusions. Although hub, mean, and tip loss characteristics obtained from surveys just downstream of each of the rotors of references 5 to 8 were correlated on the basis of design suction-surface diffusion in reference 10, the results of reference 9 indicate that, in general, correlations of this type could not be expected because of the action of rotor secondary flow in transporting the low-momentum fluids away from their original radial position. Thus, from these considerations it is indicated that a loss parameter based on over-all performance should be used in studying the loss characteristics of rotors.

An over-all loss parameter of this type is used in references 8 and 9 to correlate turbine loss on the basis of rotor surface diffusion. This loss parameter, based on over-all turbine efficiency and rotor solidity, was satisfactory for the series of transonic turbine rotors because the rotative speeds, work outputs, and weight flows were similar. Although in reference 8 the loss parameter is correlated with the suction-surface diffusion parameter, the results of reference 9 indicate that rotor design pressure-surface diffusion is also an important consideration and that improved correlation of loss could be obtained when based on the sum of the suction- and pressure-surface diffusion parameters. In view of the preceding considerations, a loss parameter based on over-all rotor performance correlated with a total surface

diffusion parameter (equal to the sum of the suction- and pressure-surface diffusion parameters) should be satisfactory in studying rotor loss characteristics. The loss parameter should, however, be independent of the operational characteristics of the turbine in order to have more general validity. Thus, a more basic parameter than that used in references 8 and 9 is desired.

This report describes the application of an effective rotor-blade momentum thickness as a more basic parameter for use in studying the loss characteristics of rotors. This momentum thickness is defined in a manner similar to that in reference 1 except that it is obtained from over-all performance characteristics instead of from blade-wake surveys. Included in this report will be (1) a description of the method used to obtain the effective rotor-blade momentum thickness using over-all turbine performance, stator performance, and rotor geometric quantities; (2) the correlation of this effective rotor-blade momentum thickness obtained for the series of transonic turbines of references 5 to 9 with design total surface diffusion; and (3) comparison of the correlation with that obtained from the low-speed two-dimensional cascade results described in reference 11.

DEVELOPMENT OF METHOD TO OBTAIN EFFECTIVE ROTOR-BLADE MOMENTUM THICKNESS

The effective rotor-blade momentum thickness developed herein is obtained from stator design-point performance, over-all turbine design-point performance, and rotor geometric quantities. In addition to the blade profile losses, the development will include the effect of inner- and outer-wall boundary-layer loss using the method of reference 3 (which is described in appendix B of this report) as well as the effect of mixing downstream of the blade rows using the method of reference 1.

Performance Characteristics and Geometric Quantities

The necessary turbine over-all performance characteristics at design point can be obtained from the performance map and measured turbine-inlet conditions. These characteristics are (1) equivalent specific work output $\Delta h'/\theta_{cr}$, (2) ratio of specific heats γ, (3) turbine-inlet total temperature T_0', (4) turbine-inlet total pressure p_0', and (5) turbine-outlet total pressure p_4'. (All symbols are defined in appendix A, and the station nomenclature is described in fig. 1.)

The outlet total temperature T_4' was calculated from the inlet total temperature and turbine work output computed from torque, speed, and weight-flow measurements. The inlet and outlet total pressures

were obtained from measured static pressures, total temperatures, weight flow, average flow angle, and annulus area using the total-to-static pressure relations given in equation (B1) of appendix B.

The necessary stator performance characteristics at design point can be obtained from stator surveys. The pertinent parameter needed for the subject analysis is the stator loss total-pressure ratio p_2'/p_0', which includes the wall losses within the stator passages as well as the nonuniformities at the blade exit but is corrected for the wall losses up to the stator leading edge.

The rotor geometric quantities used in the development are based on mean-section quantities. These quantities are (1) stagger angle α_s, (2) blade solidity σ, (3) aspect ratio based on blade chord $\mathscr{A}$, and (4) ratio of trailing-edge thickness to spacing t/s.

The parameters required from the rotor design velocity diagrams are also based on mean-section values. These parameters are (1) relative outlet critical velocity ratio $(W/W_{cr})_{fs,m,3}$ and (2) relative outlet flow angle β_3.

The rotor loss total-pressure ratio p_4''/p_2'' can be computed as follows: The over-all total-pressure ratio p_4'/p_0' can be expanded to yield

$$\frac{p_4'}{p_0'} = \frac{p_4'}{p_4''}\frac{p_4''}{p_2''}\frac{p_2''}{p_2'}\frac{p_2'}{p_0'} \tag{1}$$

Because the relative total temperature at a given radius is constant for free vortex flow and approximately so for the other types of flow, and because T_2' is equal to T_0', the following relation can be written:

$$\left(\frac{T_4'}{T_4''}\right)^{\frac{\gamma}{\gamma-1}}\left(\frac{T_2''}{T_2'}\right)^{\frac{\gamma}{\gamma-1}} = \left(\frac{T_4'}{T_0'}\right)^{\frac{\gamma}{\gamma-1}}$$

or

$$\frac{p_4'}{p_4''}\frac{p_2''}{p_2'} = \left(\frac{T_4'}{T_0'}\right)^{\frac{\gamma}{\gamma-1}} \tag{2}$$

By substituting equation (2) into equation (1) and rearranging terms, the rotor loss total-pressure ratio can be obtained from

$$\frac{p_4''}{p_2''} = \frac{p_4'/p_0'}{\frac{p_2'}{p_0'}\left(\frac{T_4'}{T_0'}\right)^{\frac{\gamma}{\gamma-1}}} \tag{3}$$

Effective Rotor-Blade Momentum Thickness

The preceding section shows how the rotor loss total-pressure ratio p_4''/p_2'' can be obtained from the over-all design performance, the turbine geometric quantities, and the stator surveys. In reference 3 a method is presented for determining the loss total-pressure ratio for a blade row based on an effective momentum thickness $\overline{\theta}_{tot}$. It is assumed in the reference that this effective momentum thickness occurred at the blade mean section and that it represented the average momentum loss per unit surface area for the blade surfaces and the end walls. In the reference method it is assumed that uniform flow enters the rotor and the loss total-pressure ratio includes the effect of flow nonuniformities at the blade exit. Thus the loss total-pressure ratio obtained by the method of reference 3 is directly comparable with the rotor loss total-pressure ratio obtained from the performance data.

The effective rotor-blade momentum thickness can be computed from the loss total-pressure ratio p_4''/p_2'' by applying the method of reference 3. In the computation it is convenient to assume a range of $\overline{\theta}_{tot}$ or preferably $\overline{\theta}_{tot}/c$. For assumed values of $\overline{\theta}_{tot}/c$, values of $\overline{\delta}_{tot}/c$ can be estimated by assuming a simple-power-law velocity profile with an exponent of 1/7 for the boundary-layer flow and by knowing the rotor-outlet relative critical velocity ratio $(W/W_{cr})_{fs,m,3}$. Although the form factor H, which relates $\overline{\theta}_{tot}/c$ and $\overline{\delta}_{tot}/c$, is approximated in this manner, it can be shown from the results of reference 1 that the loss total-pressure ratio is quite insensitive to small inaccuracies in the value of $\overline{\delta}_{tot}/c$. A curve of loss total-pressure ratio as a function of $\overline{\theta}_{tot}/c$ can then be constructed. The value of loss total-pressure ratio corresponding to that computed from the performance data then defines the ratio of effective rotor-blade momentum thickness to chord length $\overline{\theta}_{tot}/c$ from this curve. A sample calculation is included in appendix B that demonstrates this procedure.

The inlet and outlet total pressures (p_0' and p_4', respectively) used herein are recognized as being somewhat low, because equation (B1) assumes, in effect, a constant velocity throughout the flow area. In order to obtain an effective total pressure at the inlet or outlet, it would be necessary to determine the nonuniformities of the flow. The effective total pressure would then be the total pressure after mixing assuming continuity, conservation of momentum, and conservation of energy in the mixing process (see ref. 12). The error in calculating the total pressure by equation (B1) is a function of the degree of nonuniformity and the Mach number level. Therefore, the error in total pressure at the turbine inlet would be quite small because the only nonuniformities at the inlet arise from the wall boundary layers. Theoretically it can be shown that this error would be about 0.003. At the turbine outlet the error in total pressure cannot be estimated quantitatively, because the degree of flow nonuniformity is not known. However, it is felt that the calculated total pressure is reasonably accurate because the measuring station is located axially about one-third of a chord length downstream of the trailing edge. In reference 13 it is shown that a rapid mixing occurs downstream of a blade row, and it is therefore felt that by the time the flow reaches the turbine-outlet measuring station much of the mixing has occurred.

MOMENTUM-THICKNESS CORRELATIONS FOR REFERENCE TRANSONIC TURBINE ROTORS

The ratio of effective rotor-blade momentum thickness to chord length $\overline{\theta}_{tot}/c$ was calculated at the design point for the transonic turbines of references 5 to 9 and 14. The results of these calculations are presented in figure 2, where $\overline{\theta}_{tot}/c$ is presented as a function of the design total surface diffusion parameter D_{tot}. Inspection of this figure reveals that satisfactory correlation of $\overline{\theta}_{tot}/c$ with D_{tot} occurs for these rotors. The parameter $\overline{\theta}_{tot}/c$ is seen to increase somewhat linearly from approximately 0.010 at $D_{tot} = 0.35$ to 0.014 at $D_{tot} = 0.55$; thereafter the curve hooks up to approximately 0.0226 at $D_{tot} = 0.66$.

Comparison of the trend of this correlation with that obtained in reference 9 can be made from figure 3, where the specific blade loss L is presented as a function of D_{tot}. The major difference between the trends of the two correlating curves (figs. 2 and 3) occurs at high diffusions where the curve remains straight when using L as the loss parameter. The difference occurs as a result of the design requirements of the turbine of reference 6 being slightly different from those of the other reference turbines, the principal factor being the rotor-outlet velocity level.

As pointed out in the development section, it is assumed that the momentum loss is a function of the blade surface area. Also, when blades of high turning are considered (as is done herein), the chord is not representative of the average of the suction- and pressure-surface lengths (ref. 3). Thus, a length more descriptive of the surface length than c is desired when presenting momentum loss characteristics. One such length would be that of the blade mean camber line. An improved parameter would then be the ratio of effective rotor-blade momentum thickness to mean camber length $\overline{\theta}_{tot}/l$, which can be computed from the relation

$$\frac{\overline{\theta}_{tot}}{l} = \frac{\overline{\theta}_{tot}}{c}\frac{c}{l}$$

where c/l can be obtained from rotor geometry. Figure 4 presents $\overline{\theta}_{tot}/l$ as a function of D_{tot} for the reference transonic turbine rotors. The same trends that are shown in figure 2 are indicated in figure 4, but the level of the curve in figure 4 is approximately 10 percent lower because the value of c/l is approximately 0.90 for all the reference transonic turbine rotors.

COMPARISON OF MOMENTUM THICKNESSES OF TRANSONIC ROTORS WITH THOSE OF LOW-SPEED TWO-DIMENSIONAL CASCADES

A comparison of the ratios of effective rotor-blade momentum thickness to mean camber length $\overline{\theta}_{tot}/l$ obtained for the reference transonic turbine rotors with the θ_{tot}/l values obtained for a series of low-speed two-dimensional cascades is presented in figure 5. The experimental data used for the low-speed results are reported in reference 11 in terms of a wake momentum difference coefficient C_w. The method used to convert this parameter to that used in figure 5 is described in reference 10. The data points for the low-speed cascades shown in figure 5 are those obtained at approximately design turning. All these data points except two were obtained with a very low value of turbulence at the cascade inlet. The two points were obtained with a turbulence generator at the cascade inlet. The curve shown for the transonic turbine rotors is reproduced from figure 4 and hence is shown as a function of the design total surface diffusion parameter D_{tot}. The surface diffusion parameter used in plotting each low-speed cascade data point was obtained from the measured static-pressure distribution around the blade (ref. 11).

As shown by figure 5 the slopes of the two correlating curves are approximately equal over the range of total surface diffusion parameters

for the low-speed cascade tests. It should be noted, however, that there is a sharp upward trend in the curve for the transonic turbine rotors occurring at values of D_{tot} greater than those covered by the low-speed cascade tests. The correlating curve for the rotors is also seen to be higher than the curve for the low-speed cascade tests. As mentioned previously, most of the low-speed data were obtained with very low inlet turbulence, whereas the flow entering the transonic turbine rotors was highly turbulent. It is felt that the inlet turbulence is one of the most important factors affecting the momentum loss. Therefore, two points were included from reference 11 which were obtained by using a turbulence generator at the cascade inlet. As shown in figure 5, θ_{tot}/l is increased markedly by the inlet turbulence, especially at the higher value of total surface diffusion parameter. Furthermore, the values of $\overline{\theta}_{tot}/l$ obtained for the transonic turbine rotors are comparable with those obtained from the low-speed cascade blading with high inlet turbulence.

Also included in figure 5 is the value of $\overline{\theta}_{tot}/l$ obtained from the stator of reference 4 at the design point. This value was obtained with fairly turbulent inlet conditions and would therefore not be expected to agree with the curve for the cascade data of reference 11. However, the momentum loss for the stator of reference 4 agrees fairly well with that obtained from the low-speed cascade at D_{tot} of 0.085 when the turbulence generator was used at the cascade inlet.

In addition to the inlet turbulence level the following factors may affect a comparison of the transonic-turbine-rotor loss data with those obtained from the low-speed cascade:

(1) The higher flow velocities for the transonic turbine rotors may cause shock losses that would increase $\overline{\theta}_{tot}/l$.

(2) The surface diffusion parameters for the low-speed cascade blading were obtained from experimental data, whereas the D_{tot} values for the transonic-turbine-rotor blades were obtained from the design blade-loading diagrams and may differ somewhat from the actual experimental values.

(3) Due to the three-dimensional nature of the flow in the rotor passage, the losses are complicated by secondary-flow effects, such as (a) passage vortices and (b) tip clearance or scraping vortices (see ref. 15), and these additional effects may contribute to the over-all loss picture.

Although these factors may affect a comparison of these two types of blading, it is interesting to note that there is considerable

similarity in the trends of the loss curves obtained for the low-speed cascade blading and the transonic-turbine-rotor blades. Based on the limited amount of data presented, the difference in loss magnitude between the two curves (fig. 5) might well be the result of the difference in inlet turbulent level.

CONCLUDING REMARKS

This report has presented the use of an effective rotor-blade momentum thickness in describing rotor loss characteristics. This parameter was then used in correlating the rotor losses obtained for a series of transonic turbines with a design total surface diffusion parameter. Because of the inability of obtaining measured diffusions on the rotor-blade surfaces, a correlation of this type for rotors must be restricted to design point, where the diffusion characteristics are felt to be known with reasonable accuracy. When means for experimentally obtaining rotor surface diffusion characteristics are devised, this approach can then be extended to off-design regions.

Lewis Flight Propulsion Laboratory
National Advisory Committee for Aeronautics
Cleveland, Ohio, March 1, 1956

APPENDIX A

SYMBOLS

The following symbols are used in this report:

A	parameter defined by eq. (B6)
A_a	annulus area, sq ft
A_b	blade surface area, sq ft
A_w	sum of inner- and outer-wall areas within blade row, sq ft
$\mathscr{A}$	rotor aspect ratio, ratio of rotor-blade height to mean-section chord length
C	parameter defined by eq. (B7)
C_w	wake momentum difference coefficient (see ref. 11)
c	blade mean-section chord length, ft
c_p	specific heat at constant pressure, Btu/(lb)($^\circ$R)
D	blade surface diffusion parameter, $1 - \frac{\text{velocity after diffusion}}{\text{velocity before diffusion}}$
g	acceleration due to gravity, 32.17 ft/sec^2
H	form factor, δ/θ
$\Delta h'$	specific work output, Btu/lb
K	parameter defined by eq. (B8)
L	specific blade loss, $(1 - \eta)/\sigma$
l	length of blade mean camber line, ft
N	number of blades
n	exponent used in describing simple-power-law boundary-layer velocity profile

[redacted]

p	absolute pressure, lb/sq ft
R	gas constant, ft/$^{\circ}$R
r	radius, ft
s	rotor-blade spacing at mean section, ft
T	temperature, $^{\circ}$R
t	rotor-blade trailing-edge thickness at mean section, ft
V	absolute gas velocity, ft/sec
W	relative gas velocity, ft/sec
w	weight flow, lb/sec
α	absolute gas-flow angle measured from axial direction, deg
α_s	rotor-blade mean-section stagger angle measured from axial direction, deg
β	relative gas-flow angle at mean section measured from axial direction, deg
γ	ratio of specific heats
δ	displacement thickness, ft
δ_{te}	ratio of tangential projection of trailing-edge thickness to spacing, $t/s \cos \beta$
δ^*	displacement thickness, $\delta_{tot}/s \cos \beta$
$\bar{\delta}$	effective displacement thickness, ft
ε	function of γ, $\frac{\gamma_{sl}}{\gamma}\left[\frac{\left(\frac{\gamma+1}{2}\right)^{\frac{\gamma}{\gamma-1}}}{\left(\frac{\gamma_{sl}+1}{2}\right)^{\frac{\gamma_{sl}}{\gamma_{sl}-1}}}\right]$
ζ	ratio of inlet-air total pressure to NACA standard sea-level pressure, p_0'/p_{sl}

[redacted]

η adiabatic efficiency, ratio of turbine work based on torque, weight flow, and speed measurements to ideal work based on inlet total temperature, inlet total pressure, and outlet total pressure

Θ_{cr} squared ratio of critical velocity at turbine inlet to critical velocity at NACA standard sea-level temperature, $(V_{cr,0}/V_{cr,sl})^2$

θ momentum thickness, ft

$\overline{\theta}$ effective rotor-blade momentum thickness based on turbine over-all performance, ft

θ^* momentum-thickness parameter, $\theta_{tot}/s \cos \beta$

ρ gas density, lb/cu ft

σ rotor-blade mean-section solidity, c/s

Subscripts:

cr conditions at Mach number of 1.0

fs conditions in free stream or that region between blade wakes

m mean radius

r rotor

sl NACA standard sea-level conditions

tot sum of suction- and pressure-surface quantities

x axial direction

2d two dimensional

3d three dimensional

0 station upstream of turbine stator

1 station just downstream of stator trailing edge

2 station at rotor entrance

3 station just downstream of rotor trailing edge

[redacted]

4 station downstream of rotor where circumferentially uniform conditions are assumed to exist

Superscripts:

' absolute total state

" relative total state

[redacted]

APPENDIX B

EXAMPLE CALCULATION OF EFFECTIVE MOMENTUM THICKNESS FOR TURBINE ROTORS

The general development of the method used to calculate an effective momentum thickness for rotors is given in the body of the report. Further details of the method are given in the following example.

Required Performance, Design, and Geometric Quantities

The performance, design, and geometric quantities required to calculate an effective rotor-blade momentum thickness are

Equivalent specific work output, $\Delta h'/\theta_{cr}$, Btu/lb	23.03
Ratio of specific heats, γ	1.4
Specific heat at constant pressure, c_p	0.24
Inlet total temperature, T_0', $^\circ R$	518.7
Equivalent weight flow, $w\varepsilon\sqrt{\theta_{cr}}/\zeta$, lb/sec	11.95
Inlet total pressure, p_0', lb/sq ft	2116.2
Rotor-blade stagger angle, α_s, deg	12.5
Rotor-blade solidity, σ	1.816
Rotor-blade aspect ratio, $\mathscr{A}$	0.773
Rotor-blade trailing-edge thickness, t, in.	0.030
Number of rotor blades, N	25
Rotor mean-section radius, r_m, in.	5.95
Rotor-exit relative flow angle, β_3, deg	41.0
Rotor-exit relative critical velocity ratio, $(W/W_{cr})_{fs,m,3}$	1.02
Outlet total pressure, p_4', lb/sq ft	916.3

Calculation of Rotor Loss Total-Pressure Ratio

The stator-inlet total pressure p_0' was calculated on the basis of continuity from the inlet static pressure p_0 (averaged from static pressures measured at the hub and tip), measured inlet total temperature T_0', measured weight flow w, and the annulus area A_a by using equation (2) of reference 16 rearranged in the following form:

$$\left\{\left[\left(\frac{p'}{p}\right)_0^{\frac{\gamma-1}{\gamma}} - 1\right]^2 + \left[\left(\frac{p'}{p}\right)_0^{\frac{\gamma-1}{\gamma}} - 1\right]\right\}^{1/2} \left[\frac{2g\gamma}{(\gamma-1)R}\right]^{1/2} = \frac{w\sqrt{T_0'}}{p_0 A_a \cos\alpha_0} \tag{B1}$$

[redacted]

The right side of equation (B1) is divided by $\cos \alpha_0$ in order that the product $A_a \cos \alpha_0$ would represent the area perpendicular to the flow. For this example p_0' is 2116.2 pounds per square foot and T_0' is 518.7° R (standard sea-level conditions); therefore, the symbols defining equivalent conditions are hereinafter dropped from the equations.

The average turbine-outlet total temperature was then obtained from $T_4' = T_0' - \Delta h'/c_p = 422.7°$ R.

The average turbine-outlet static pressure p_4 was obtained in a manner similar to that for the turbine inlet, and the outlet total pressure p_4' was calculated from equation (B1). The resulting turbine overall total-pressure ratio was

$$\frac{p_4'}{p_0'} = 0.433$$

The stator of this example turbine is described in reference 14. The reported stator loss total-pressure ratio, which included the wall losses within the stator passage as well as the effect of the nonuniformities at the blade exit but was corrected for the wall losses up to the stator leading edge, was

$$\frac{p_2'}{p_0'} = 0.970$$

at a design $(V/V_{cr})_{fs,m,l}$ of 1.11. Because the turbine-inlet and -outlet total pressures were calculated on the basis of continuity in the manner previously outlined, the loss in total pressure along the inner and outer walls upstream of the stator leading edge was not included; therefore, the stator loss total-pressure ratio was corrected for the wall loss.

The rotor loss total-pressure ratio can be calculated from

$$\frac{p_4''}{p_2''} = \frac{p_4'/p_0'}{\frac{p_2'}{p_0'}\left(\frac{T_4'}{T_0'}\right)^{\frac{\gamma}{\gamma-1}}} \tag{3}$$

to be 0.912.

[redacted]

Determination of Effective Rotor-Blade Momentum Thickness

A method of calculating a loss total-pressure ratio for a three-dimensional blade row from conditions at the trailing edge of the blade mean section is presented in reference 3. Because velocity profiles at the rotor trailing edge are not experimentally obtainable at present, it is necessary to determine by iteration a ratio of effective momentum thickness to chord length $\overline{\theta}_{tot}/c$ at the mean section that will result in the rotor loss total-pressure ratio equal to that calculated from performance data. In the actual calculation for this example turbine, a range of values of $\overline{\theta}_{tot}/c$ were assumed and corresponding values of rotor loss total-pressure ratio p_4''/p_2'' were calculated. Then the value of $\overline{\theta}_{tot}/c$ corresponding to the value of p_4''/p_2'' in equation (3) was obtained from figure 6. However, for this example, the value of $\overline{\theta}_{tot}/c$ of 0.0138 corresponding to the calculated p_4''/p_2'' of 0.912 (see fig. 6) was chosen in order to eliminate the iteration process.

The method of reference 3 for calculating a loss total-pressure ratio requires that the effective momentum thickness $\overline{\theta}_{tot}$ and the trailing-edge thickness t be expressed in terms of tangential values per unit of blade spacing. The corresponding momentum-thickness parameter is given by

$$\theta^*_{r,2d} = \frac{\overline{\theta}_{tot}}{s \cos \beta_3} = \frac{\overline{\theta}_{tot}}{c} \frac{\sigma}{\cos \beta_3} = 0.0332 \qquad (B2)$$

The momentum-thickness parameter has to be modified to obtain an equivalent three-dimensional expression which includes the effects of the end walls of the blade passage. In reference 3 the ratio of the three-dimensional area to the two-dimensional area was approximated by

$$(A_b + A_w)/A_b = 1 + \cos \alpha_s/\sigma \qquad (B3)$$

Thus, with the assumed momentum loss distribution over the end walls and the blade surfaces, $\theta^*_{r,2d}$ of equation (B2) can be modified to a three-dimensional value by

$$\theta^*_{r,3d} = \theta^*_{r,2d} \left(1 + \frac{\cos \alpha_s}{\sigma}\right) = 0.0563 \qquad (B4)$$

As pointed out in reference 3, the blockage due to the trailing-edge thickness, expressed as a percentage of the total flow area, would be the same for the three-dimensional concept as for the two-dimensional case. Thus,

$$\delta_{te,r,2d} = \delta_{te,r,3d} = \frac{t}{s \cos \beta_3} = 0.0266 \tag{B5}$$

An approximate value of the three-dimensional displacement-thickness parameter $\delta^*_{r,3d}$ required in the method of reference 3 can be calculated from $\theta^*_{r,3d}$ and a theoretical form factor H for a simple-power-law velocity profile having an exponent n of 1/7 as discussed in this report. Therefore, from figure 7 (which is fig. 4 of ref. 3), which gives H as a function of the free-stream critical velocity ratio, H = 1.76 for $(W/W_{cr})_{fs,m,3}$ of 1.02. Thus,

$$\delta^*_{r,3d} = H\theta^*_{r,3d} = 0.0991$$

The values for $\theta^*_{r,3d}$, $\delta^*_{r,3d}$, $\delta_{te,r,3d}$, β_3, and $(W/W_{cr})_{fs,m,3}$ were used to compute p''_4/p''_2 by substitution in equations (B4), (C16), (C18), (C20), (C21), and (C22) of reference 1, which are rewritten herein with the symbols of this report:

$$A \equiv \frac{\gamma - 1}{\gamma + 1}\left(\frac{W}{W_{cr}}\right)^2_{fs,m,3} = 0.173 \tag{B6}$$

$$C \equiv \frac{(1 - A)\left(\frac{\gamma + 1}{2\gamma}\right) + \cos^2\beta_3 \left(1 - \delta^*_{r,3d} - \delta_{te,r,3d} - \theta^*_{r,3d}\right)\left(\frac{W}{W_{cr}}\right)^2_{fs,m,3}}{\cos \beta_3 \left(1 - \delta^*_{r,3d} - \delta_{te,r,3d}\right)\left(\frac{W}{W_{cr}}\right)_{fs,m,3}}$$

$$= 1.773 \tag{B7}$$

$$K \equiv \left(\frac{W}{W_{cr}}\right)_{fs,m,3} \sin \beta_3 \left(\frac{1 - \delta^*_{r,3d} - \delta_{te,r,3d} - \theta^*_{r,3d}}{1 - \delta^*_{r,3d} - \delta_{te,r,3d}}\right) = 0.626 \tag{B8}$$

$$\left(\frac{W_x}{W_{cr}}\right)_4 = \frac{\gamma C}{\gamma + 1} - \sqrt{\left(\frac{\gamma C}{\gamma + 1}\right)^2 - 1 + \frac{\gamma - 1}{\gamma + 1} K^2} = 0.667 \qquad (B9)$$

$$\left(\frac{\rho}{\rho''}\right)_4 = \left\{1 - \frac{\gamma - 1}{\gamma + 1}\left[K^2 + \left(\frac{W_x}{W_{cr}}\right)_4^2\right]\right\}^{\frac{1}{\gamma - 1}} = 0.687 \qquad (B10)$$

$$\frac{p_4''}{p_2''} = \frac{\left(\frac{\rho W}{\rho'' W_{cr}}\right)_{fs,m,3} \cos \beta_3 \, (1 - \delta^*_{r,3d} - \delta_{te,r,3d})}{\left(\frac{\rho W_x}{\rho'' W_{cr}}\right)_4} = 0.912 \qquad (B11)$$

3923

REFERENCES

1. Stewart, Warner L.: Analysis of Two-Dimensional Compressible-Flow Loss Characteristics Downstream of Turbomachine Blade Rows in Terms of Basic Boundary-Layer Characteristics. NACA TN 3515, 1955.

2. Whitney, Warren J., Stewart, Warner L., and Miser, James W.: Experimental Investigation of Turbine Stator-Blade-Outlet Boundary-Layer Characteristics Compared with Theoretical Results. NACA RM E55K24, 1956.

3. Stewart, Warner L., Whitney, Warren J., and Wong, Robert Y.: Use of Mean-Section Boundary-Layer Parameters in Predicting Three-Dimensional Turbine Stator Losses. NACA RM E55L12a, 1956.

4. Miser, James W., Stewart, Warner L., and Wong, Robert Y.: Effect of Reduction in Stator Solidity on Performance of a Transonic Turbine. NACA RM E55L09a, 1956.

5. Stewart, Warner L., Wong Robert Y., and Evans, David G.: Design and Experimental Investigation of Transonic Turbine with Slight Negative Reaction Across Rotor Hub. NACA RM E53L29a, 1954.

6. Wong, Robert Y., Monroe, Daniel E., and Wintucky, William T.: Investigation of Effect of Increased Diffusion of Rotor-Blade Suction-Surface Velocity on Performance of Transonic Turbine. NACA RM E54F03, 1954.

[redacted]

7. Whitney, Warren J., Monroe, Daniel E., and Wong, Robert Y.: Investigation of Transonic Turbine Designed for Zero Diffusion of Suction-Surface Velocity. NACA RM E54F23, 1954.

8. Whitney, Warren J., Wong, Robert Y., and Monroe, Daniel E.: Investigation of a Transonic Turbine Designed for a Maximum Rotor-Blade Suction-Surface Relative Mach Number of 1.57. NACA RM E54G27, 1954.

9. Miser, James W., Stewart, Warner L., and Monroe, Daniel E.: Effect of High Rotor Pressure-Surface Diffusion on Performance of a Transonic Turbine. NACA RM E55H29a, 1955.

10. Wong, Robert Y., and Stewart, Warner L.: Correlation of Turbine-Blade-Element Losses Based on Wake Momentum Thickness with Diffusion Parameter for a Series of Subsonic Turbine Blades in Two-Dimensional Cascade and for Four Transonic Turbine Rotors. NACA RM E55B08, 1955.

11. Dunavant, James C., and Erwin, John R.: Investigation of a Related Series of Turbine-Blade Profiles in Cascade. NACA RM L53G15, 1953.

12. Wyatt, DeMarquis D.: Analysis of Errors Introduced by Several Methods of Weighting Nonuniform Duct Flows. NACA TN 3400, 1955.

13. Lieblein, Seymour, and Roudebush, William H.: Theoretical Loss Relations for Low-Speed Two-Dimensional-Cascade Flow. NACA TN 3662, 1956.

14. Whitney, Warren J., Stewart, Warner L., and Wong, Robert Y.: Effect of Reduced Stator-Blade Trailing-Edge Thickness on Over-All Performance of a Transonic Turbine. NACA RM E55H17, 1955.

15. Allen, Hubert W., and Kofskey, Milton G.: Visualization Study of Secondary Flows in Turbine Rotor Tip Regions. NACA TN 3519, 1955.

16. Stewart, Warner L., Schum, Harold J., and Whitney, Warren J.: Investigation of Turbine for Driving Supersonic Compressors. I - Design and Performance of First Configuration. NACA RM E52C25, 1952.

[redacted]

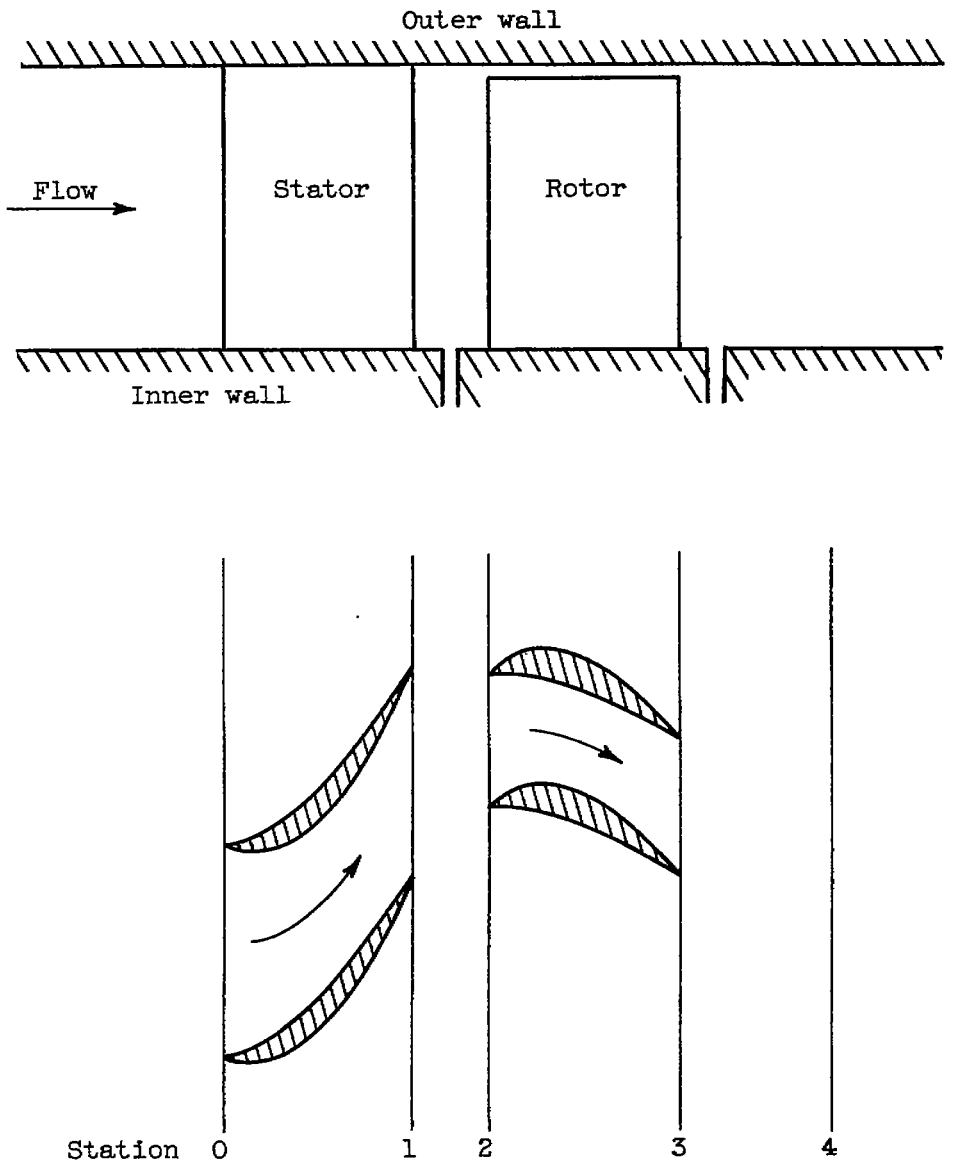

Figure 1. - Description of turbine and station nomenclature.

[redacted]

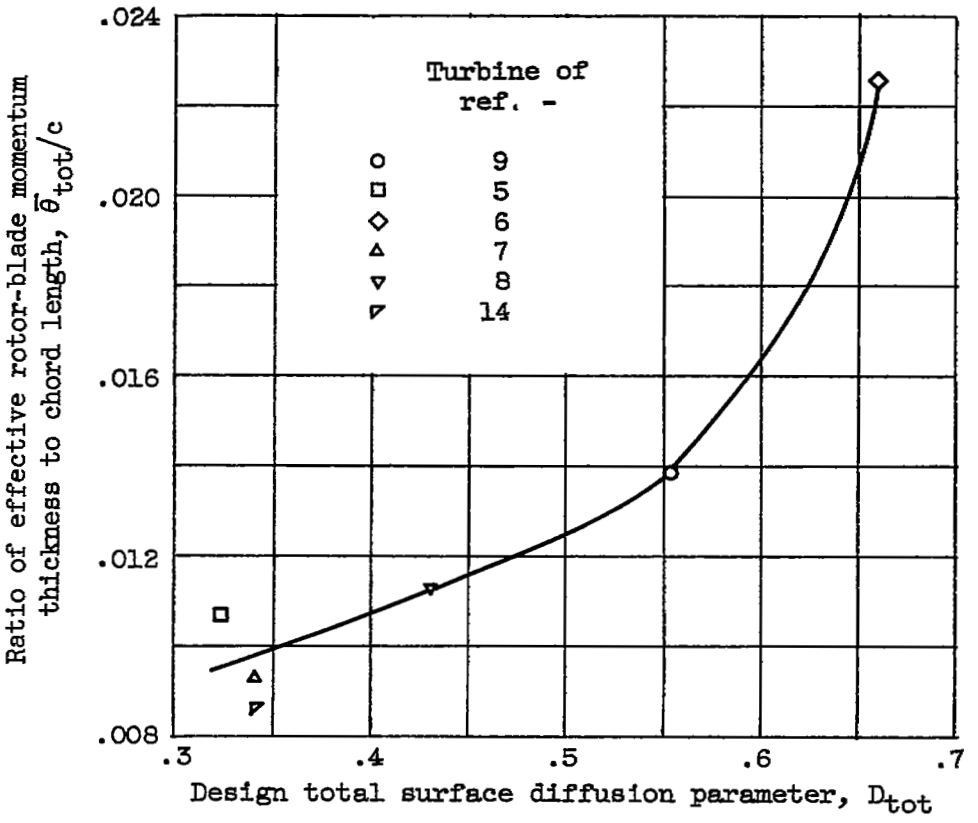

Figure 2. - Variation in ratio of momentum thickness to chord length with surface diffusion for reference transonic turbines.

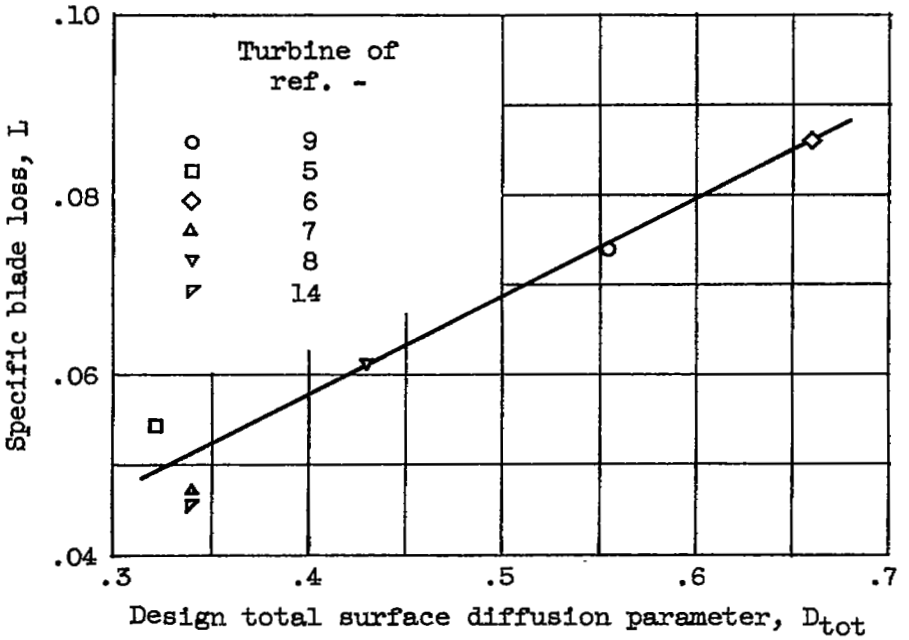

Figure 3. - Variation in specific blade loss with design total surface diffusion parameter for reference transonic turbines.

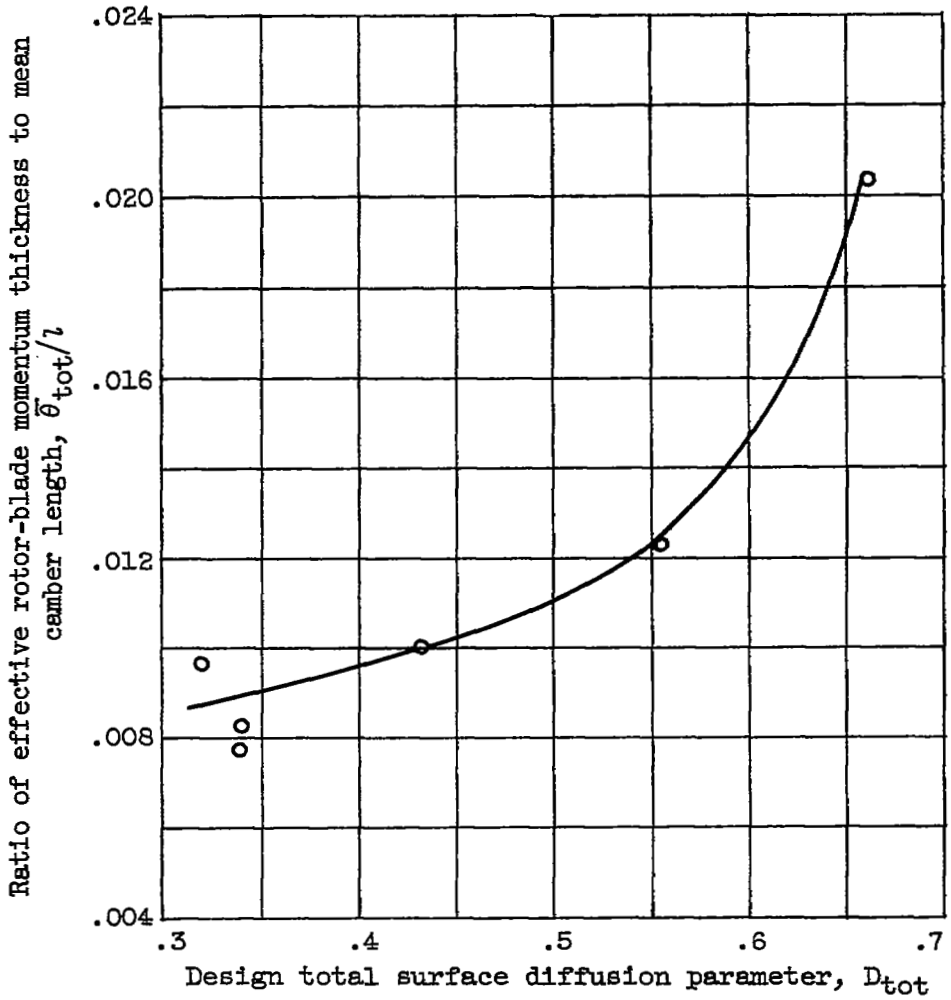

Figure 4. - Variation in ratio of effective rotor-blade momentum thickness to mean camber length with design total surface diffusion parameter.

[redacted]

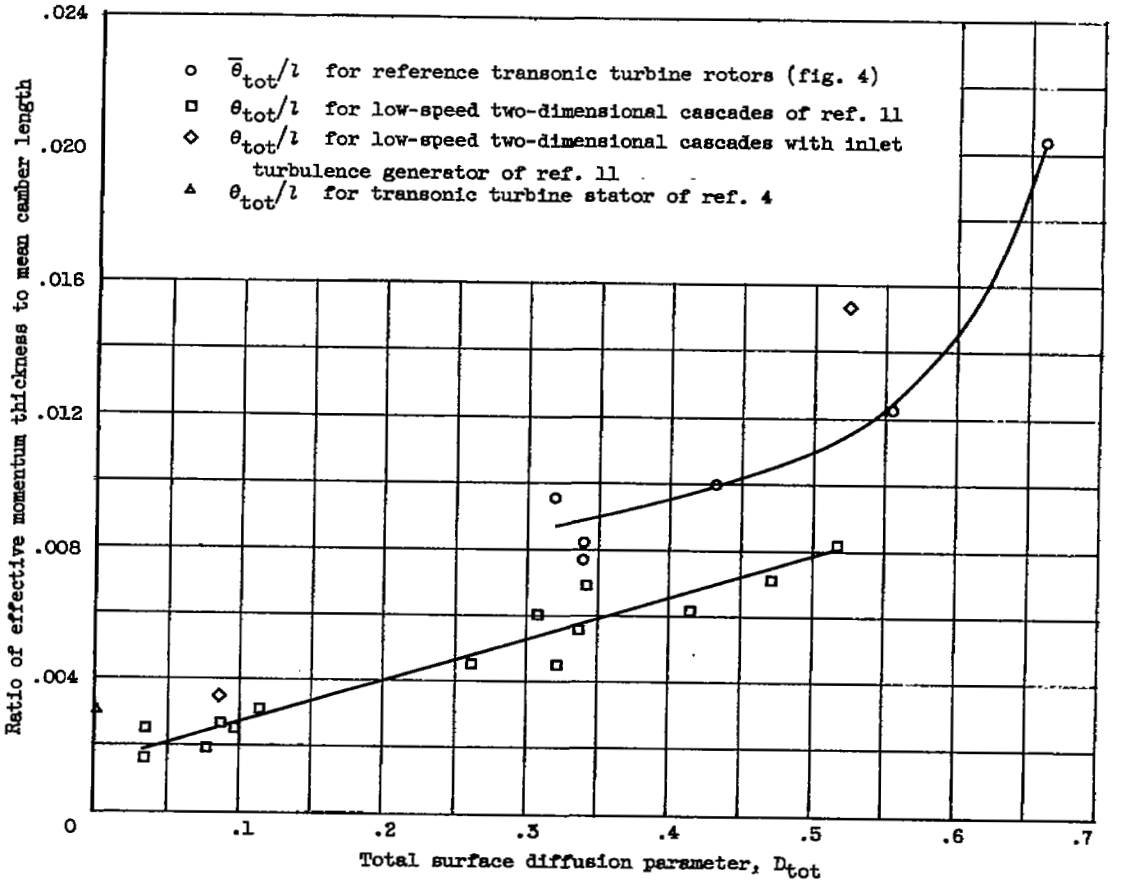

Figure 5. - Variation in ratio of effective momentum thickness to mean camber length with total surface diffusion parameter.

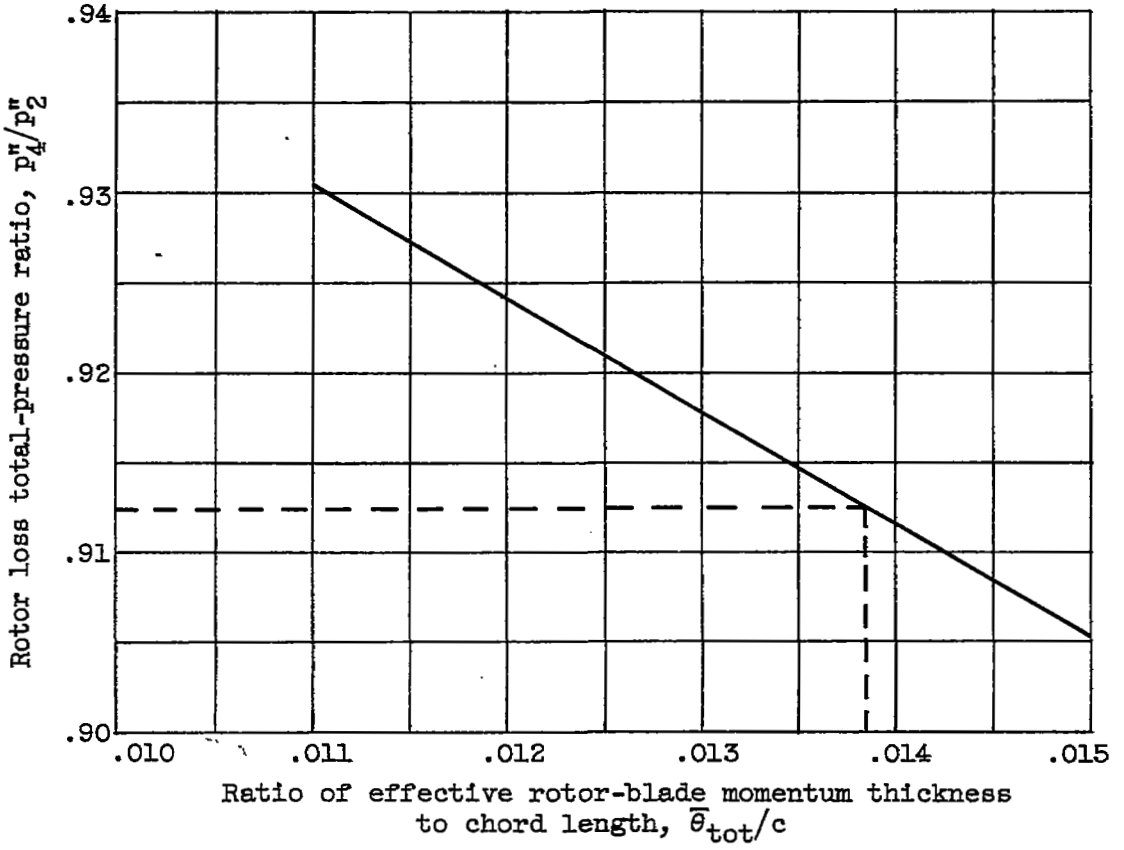

Figure 6. - Variation of rotor loss total-pressure ratio with ratio of effective rotor-blade momentum thickness to chord length.

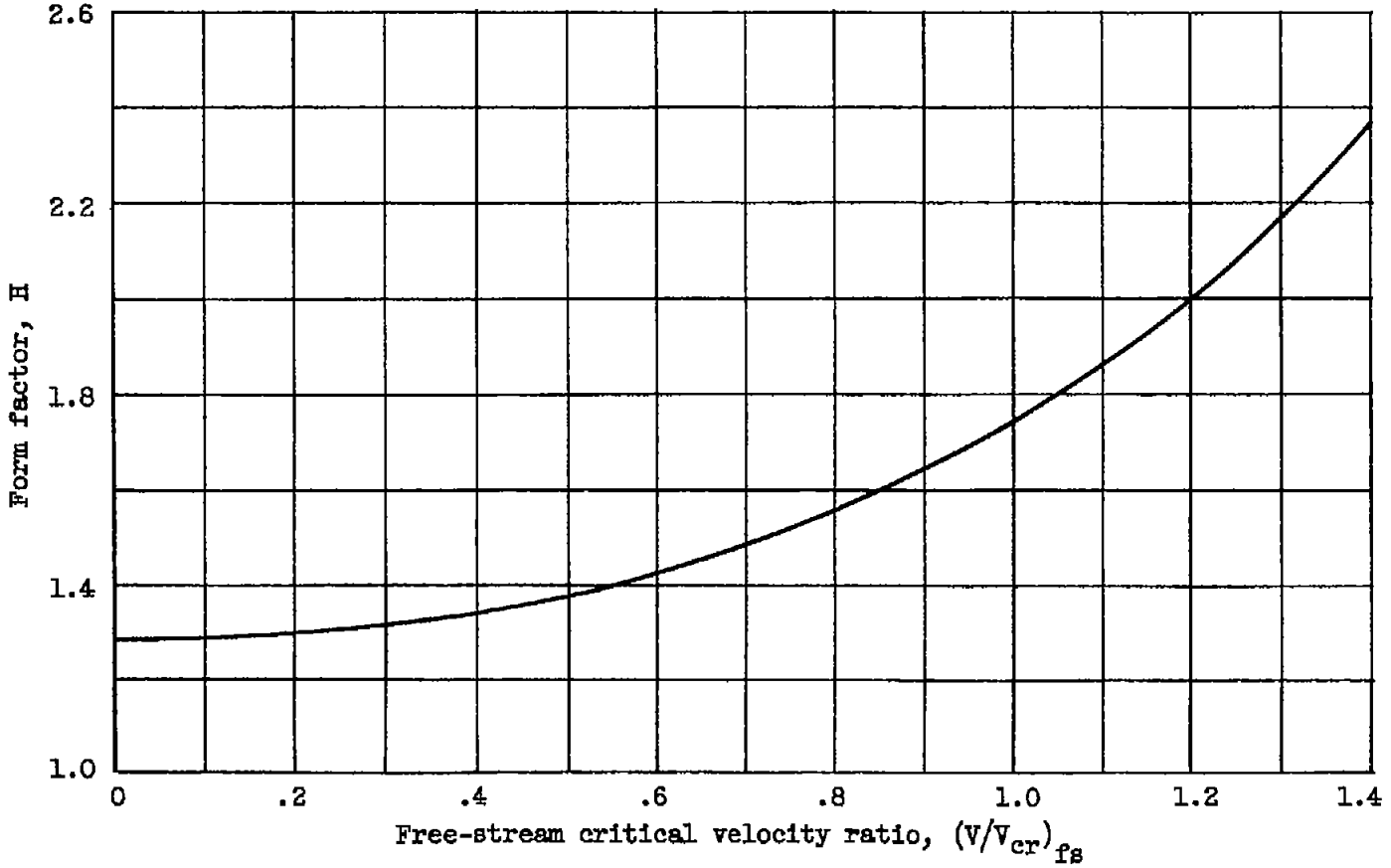

Figure 7. - Variation in form factor H with free-stream critical velocity ratio for simple-power-law velocity profile having exponent n = 1/7 (fig. 4 of ref. 3).